

## NONLINEARITY OF CONDUCTOR BEHAVIOR IN THE CONTEXT OF LOADS ON TRANSMISSION TOWERS

Grzegorz WANDZIK <sup>a\*</sup> and Grzegorz KOWALCZYK <sup>b</sup>

<sup>a</sup> Assoc. Prof. PhD, DSc; Department of Structural Engineering, Faculty of Civil Engineering, Silesian University of Technology, Gliwice  
ORCID: 0000-0002-4355-6290

\*E-mail address: [grzegorz.wandzik@polsl.pl](mailto:grzegorz.wandzik@polsl.pl)

<sup>b</sup> MSc; Arinet sp. z o.o., Gliwice  
ORCID: 0009-0005-1233-7561

Received: 26.09.2024; Revised: 11.11.2024; Accepted: 12.11.2024

### Abstract

The article presents the issue of determining the effects of conductors on the supporting structures of power lines using two different methods of applying partial safety factors (PSF). An assessment of the nonlinearity and disproportionality in the relationship between the conductor load and the tension force was carried out. The discussion identifies the source of differences in the approaches and assesses the impact of two primary factors: the curvature of the relationship between load and tension force, and the initial prestressing of the cable, which results in the displacement of the graph relative to the origin of the coordinate system. The investigation utilizes measures of nonlinearity to facilitate its assessment. A sensitivity analysis was performed to examine the difference between applying PSFs to actions and their effects. A series of numerical calculations, considering various spans, initial tensions, and load values, demonstrated the scale of the reduction in the design values of forces when safety factors are applied more naturally to the actions, not to their effects.

**Keywords:** Cable structures; High-voltage towers; Nonlinear response; Partial safety factors; Sensitivity analysis; Structure reliability.

### 1. INTRODUCTION

For the design of support structures for power lines, the limit state method based on partial safety factors (PSF) has been used for many years. The dominant actions on these towers are forces originating from the non-linear behavior of conductors. It is well known that the application of PSF in non-linear problems raises certain interpretational doubts. Therefore, the issue of determining the forces exerted by the conductors on the structure and partial factors use should receive due attention.

For over a decade, the design principles for power lines in EU countries have been governed by successive editions of the EN 50341-1 [1, 2] standard. Specific rules for Poland are defined in extensive national normative appendices NNA 2010 [3] and

NNA 2016 [4]. Due to the diverse climatic conditions in various EU countries and the differing traditions [5], most detailed guidelines are provided in the NNA editions.

One of the key issues defined in the standards is the method of ensuring the appropriate level of safety for the line and its components. In the limit states method, this is achieved using a semi-probabilistic approach that employs partial safety factors (PSF)  $\gamma$  and combination factors  $\psi$ . In the 2016 edition of the national annex for Poland, NNA 2016 [4], the concept of ensuring structural reliability was changed compared to the NNA 2010 [3]. Reliability classes were introduced, loading arrangements on towers were modified, and the values of partial factors were adjusted. One of the changes concerns the method of

applying load factors. In NNA 2010, an empirical approach was adopted, recommending the use of safety factors directly for effects (e.g., forces in conductors). In later editions, elements of a general approach were introduced (NNA 2016), recommending the direct application of factors to the loads.

Due to the nonlinearity of the relationship between the load (e.g., conductor loading, temperature change) and its effects (e.g. conductor tension force and its sag), the stage at which partial safety factors are applied is significant. The importance of this change was the focus of the analyses and discussions presented in this article.

The motivation for the analyses discussed was the work on the UMKW (polish abbreviation stand for *Universal Modular Support Structures*) used as a temporary supporting structures [6] for power lines. These structures are intended to replace sections of existing lines and typically require that their reliability level match that of the original line design (including adherence to the same standards). This means that even old standards replaced by newer editions continue to be relevant. Broader analyses (beyond the scope of this article) have addressed the issue of applying partial factors in conductor analysis together with standard load cases for towers. Here analyses were focused on evaluating the differences arising from applying these factors to either the loads (mechanical loads) or their effects (tension forces).

## 2. OBJECTIVES, SCOPE AND METHODOLOGY OF ANALYSIS

### 2.1. Objectives

The article presents the results of computational analyses related to the development of software for designing UMKW modular towers [7]. The primary objective is the nonlinear analysis of conductors, focusing on the methodology for determining the design values of conductor impacts on towers and the discrepancies resulting from varying approaches to applying partial safety factors to effects or actions (mechanical loads).

### 2.2. Scope

The publication briefly addresses the treatment of nonlinear issues in structural design. It starts with an overview and classification of the nonlinearity types in general, then focuses on conductors transferring forces to support structures. Subsequently, it examines issues of concave curvature and nonproportion-

ality in the load-tension force relationship. This section aims to clarify the nature of the problem and identify the sources of discrepancies related to recommended approaches.

The main part of the article presents the results of numerous calculations performed for typical conductors used in 110 kV lines. The primary aim was to directly compare the increase in the design value of the effect (tension force  $H_d$ ) relative to the characteristic force  $H_k$  depending on the approach used. Calculations were conducted using proprietary software [7] based on numerical methods. To provide a comprehensive view, calculations were performed for conductors in spans ranging from 200 to 400 meters and with different initial tensions  $H_0$  ranging from 12 to 24 kN.

For clarity and to isolate specific effects, uniform partial safety factors were assumed for both loads and effects ( $\gamma_A = \gamma_E = 1.3$ ). In the final section, the analysis was extended by incorporating the factors recommended in NNA 2016 [4].

### 2.3. Methodology

The analysis was based on the steel-aluminum conductor AFL 6-240 mm<sup>2</sup>, which is commonly used in overhead lines with a voltage of 110 kV. The determination of tension forces was carried out using methods employed in practical design, assuming constant axial stiffness of the conductor. Due to the use of numerical methods, it was necessary to perform a series of calculations and present their results in the form of numerical data and discretized graphs. The conductor mentioned above, in a span of  $L = 200$  m, initially tensioned to a force of  $H_0 = 18$  kN at  $T = 10^\circ\text{C}$ , served as the so-called baseline example. Since additional loads are usually associated with icing, a significant portion of the analysis was conducted at a temperature of  $-5^\circ\text{C}$ , when the icing process is most intense. Whenever analysis parameters were altered, this was indicated in the text and on the graphs.

## 3. NONLINEARITY AND PARTIAL SAFETY FACTOR METHOD

### 3.1. General classification of nonlinearity in structural design

Most modern structural design codes are based on partial safety factor (PSF) concept. These factors are easy in use for linear problems, but deliver some doubts when applied to nonlinear phenomena.

In structural design, the terms “linear” or “nonlin-

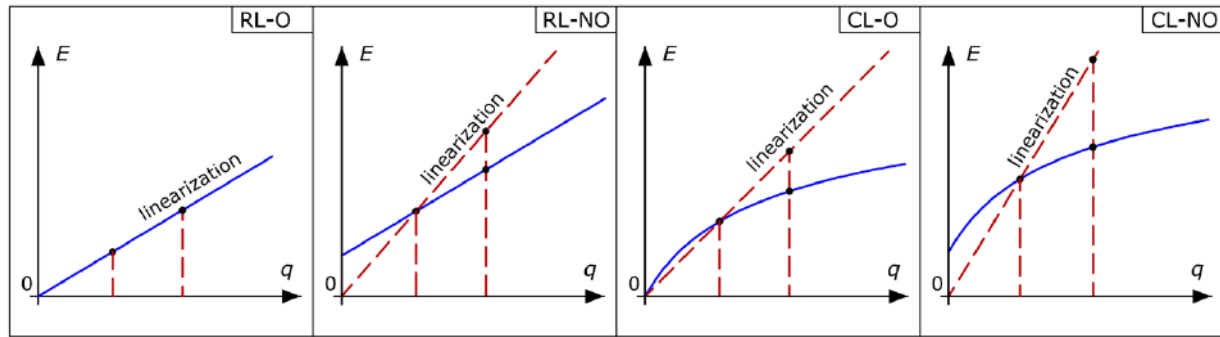


Figure 1.  
Various forms of linear/nonlinear relations  $E(q)$

ear” problem refers to relationship between actions and their effects. In linear problems, the ratio of the action effect  $E(q)$  to the action  $q$  itself is constant, satisfying the relation:

$$\frac{E(q)}{q} = \text{const} \quad (1)$$

When condition (1) is not met, the phenomenon under consideration is regarded as nonlinear. Generally, two primary sources of nonlinearity can be: significant changes in the structure’s geometry under load or changes in material properties.

Taking a broader view of the problem, one can also consider the straightness of the relationship  $E(q)$  itself and its proportionality to the origin of the coordinate system. It is possible that, while the relationship  $E(q)$  forms a straight line, it does not pass through the origin. This occurs in pre-stressed elements. Examples of various relationships between actions and their effects are shown in Figure 1. Referring to linear algebra and introducing the concept of homogeneity, the relationships  $E(q)$  can be classified as follows (with the following abbreviations):

- a) rectilinear, origin-intercept (RL-O),
- b) rectilinear, non-origin-intercept (RL-NO),
- c) curvilinear, origin-intercept (CL-O),
- d) curvilinear, non-origin-intercept (CL-NO).

Only the first of the mentioned cases satisfies the proportionality assumptions according to formula (1). All the others should be classified as nonlinear or nonproportional.

In the limit state method, reliability is ensured by using partial safety factors  $\gamma$ . In linear problems (RL-O), it does not matter whether the partial factor is applied to increase the action or its effect. Finally, the design value of the effect will be the same. In nonlinear problems, using the partial safety factor for actions or effects leads to different final effect values. The extent of these differences is determined by the

following two characteristics of the  $E(q)$  relationship:

- The distance from the origin of the coordinate system to the intersection of the  $E(q)$  curve with the ordinate axis (result of pre-stressing),
- The curvature of the  $E(q)$  relationship itself.

Simplifying by linearizing the calculation of design effects from their characteristic values (see Fig. 1), additional factors impact the final results:

- The distance of the reference point  $(q_k, E_k)$  from the origin of the coordinate system,
- The value of the partial safety factor ( $\gamma$ ).

In the Figure 1, in addition to various types of nonlinear relationships, the effect of their linearization is also shown, which occurs when applying PSF to the effects of actions.

Nonlinearity is often classified [8] as OP (over-proportional) or UP (under-proportional), depending on whether the effect increases faster (OP) or slower (UP) than the load. EN 1990:2002 [9], which defines general safety principles for building structures, suggests a conservative approach for nonlinear issues (section 6.3.2), i.e., applying load factors at such a stage that the design effect achieves a higher value. This principle is also clarified in the background document *Designers’ Guide to Eurocode: Basis of Structural Design* [10].

In the literature [11, 12, 13, 14, 15, 16], several concepts for measuring nonlinearity have been proposed. Some of these were developed for use with the partial safety factor method [8, 16], introducing indicators to quantify nonlinearity. One such indicator is an  $n$  introduced by Uhlemann [16] and further investigated by Bakker [8] (included in the *Eurocode Prospect for European Guidance for the Structural Design of Tensile Membrane Structures* [17]). The indicator proposed by Uhlemann has been also used in this study and is denoted as  $n_E$ .

### 3.2. Nonlinearity in the design of supporting structures for power lines

Nonlinearity in the design of supporting structures is associated with the behavior of cables. The lack of proportionality between actions and tension force arises from the cable's geometry, specifically the changing shape of the sagging line and its initial tension. The relationship between geometry and tension force is explored by solving the so-called *state equation*. For precise shape representation using a catenary curve, calculations are performed with numerical methods [18]. The methodology for finding the solution is well-established. The difference may lie in determining the **design values** of the tension force. As previously mentioned, according to NNA 2010 (empirical approach), the effect values are increased posterior to cable analysis, while NNA 2016 (mixed general/empirical approach) recommends increasing the action values prior to cable analysis. The procedures are briefly illustrated in Figure 2.

In the following sections of the article, the terms *Approach E* and *Approach A* are used, referring respectively to “Effect” and “Action”. The same letter symbols are used to distinguish the partial coefficients associated with these approaches. Transitioning from NNA 2010 to NNA 2016 not only changed the stage at which partial safety factors (PSFs) are considered but also their values. For this reason, an intermediate approach A was distinguished (see Figure 2), where the value of the partial safety factor is maintained as in approach E.

Approach A (**Intermediate**) differs from Approach A (NNA 2016) in the values of partial factors. The NNA 2016 variant is discussed only in the final part of the article and is designated by the symbol **A2**. To highlight the differences arising from applying PSF to

effects and actions, efforts were made to maintain identical values for these factors ( $\gamma_E = \gamma_A = 1.3$ ). Consequently, this work primarily compares Approach E (NNA 2010) and Approach A (intermediate). Therefore, any references to Approach A in the text pertain to the (intermediate) variant.

It is worth noting that the recommendations of Eurocode 0 do not apply to the design of power lines. The standards used for designing power lines structures are not a part of the Eurocodes system. Even though Eurocode 3 [19] is referenced for determining the load-bearing capacity of structural elements, Eurocode 0 [9] has been explicitly excluded as a source of information on structural safety assurance. Therefore, the previously mentioned principle of conservatively adopting safety factors does not apply to power lines design. Instead, the requirements set out in the national annexes to the PN-EN 50341-1 standard [3, 4] apply, as illustrated in Figure 2.

In general, the nonlinearity of cable behavior is not neglected. It is considered by solving the problem using the state equation. The only instance where nonlinearity might be ignored through some kind of linearization is during the determination of the design value of tension force using Approach E. Statement about linearization seems justified, considering that the uncertainty actually pertains to the values of actions rather than the method of calculating tension force. This will be discussed in more detail later in the article.

It is important to emphasize that the national annexes for Poland are not entirely precise regarding the specific application of partial safety factors, leaving some room for interpretation. In these analyses, the most conservative version of Approach E was assumed, where the factor  $\gamma_E$  (referred to as  $\gamma_C$  in the standard, from the word “conductor”) is used to

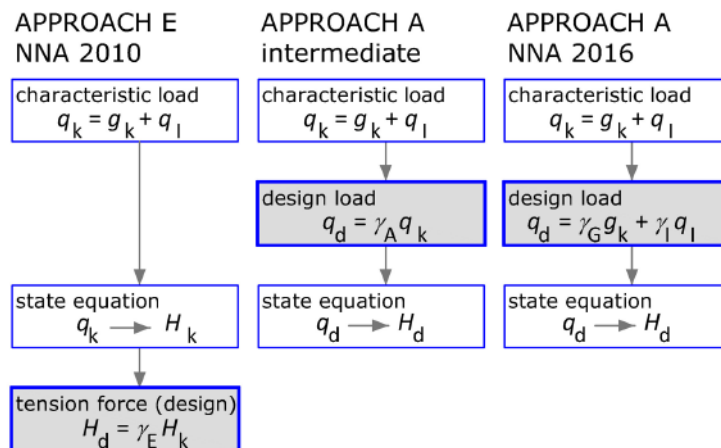


Figure 2. Diagram illustrating approaches related to PSF application for design tension forces



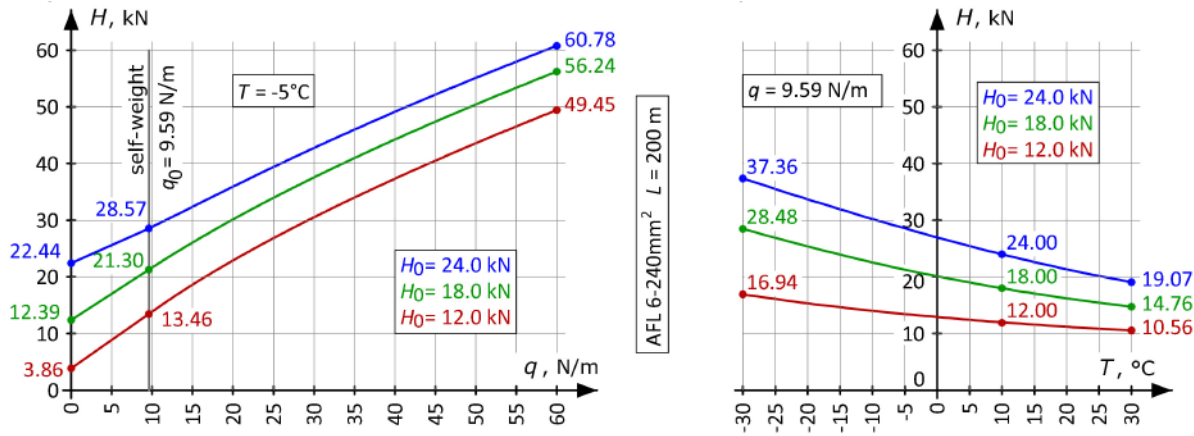


Figure 3. Relationships  $H(q)$  and  $H(T)$  for conductor AFL-6 240 mm<sup>2</sup>

uniformly increase the effect without distinguishing between the types of actions leading to it. A more detailed discussion of these issues can be found in comprehensive monographs on the design of power lines supporting structures [20, 21].

Nonlinearity in power line design pertains to determining the effects of cables on towers, primarily concerning the relationship between the horizontal component of cable tension  $H$  and the vertical load  $q$  (resulting from ice accumulation). The vertical component of the cable reaction on the supporting towers  $V$ , typically increases proportionally with changes in the load. A small exception from this rule may be found for strongly inclined spans, in which, due to the shift of the lowest point of the cable's sag, the reaction forces  $V$  at the opposite ends of the span changes slightly non-proportionally. However, the significance of the component  $V$  is much less than that of the component  $H$  and its analysis is omitted.

### 3.3. Basic relationships between actions and effects for cables

Considerations of the nonlinearity in the  $H(q)$  relationship should start with presenting an example relationship between load  $q$  and force  $H$  (Fig. 3a), complemented by a graph (Fig. 3b) showing the relationship between temperature  $T$  and force  $H$  and. The graphs were prepared for three different initial tensions of  $H_0 = 12.0, 18.0,$  and  $24.0$  kN. Figure 3a was created assuming a temperature of  $T = -5^\circ\text{C}$ , while Figure 3b was prepared for a vertical load equal to the self-weight of the cable,  $q_0 = 9.59$  N/m.

The relationship  $H(q)$  is physically meaningful for loads greater than the self-weight of the cable  $q \geq q_0$ . However, to better illustrate the issue, a portion of the graph was also created for “fictitious loads” — less than  $q_0$  (simulated by applying an additional upward load). The purpose of this approach was to

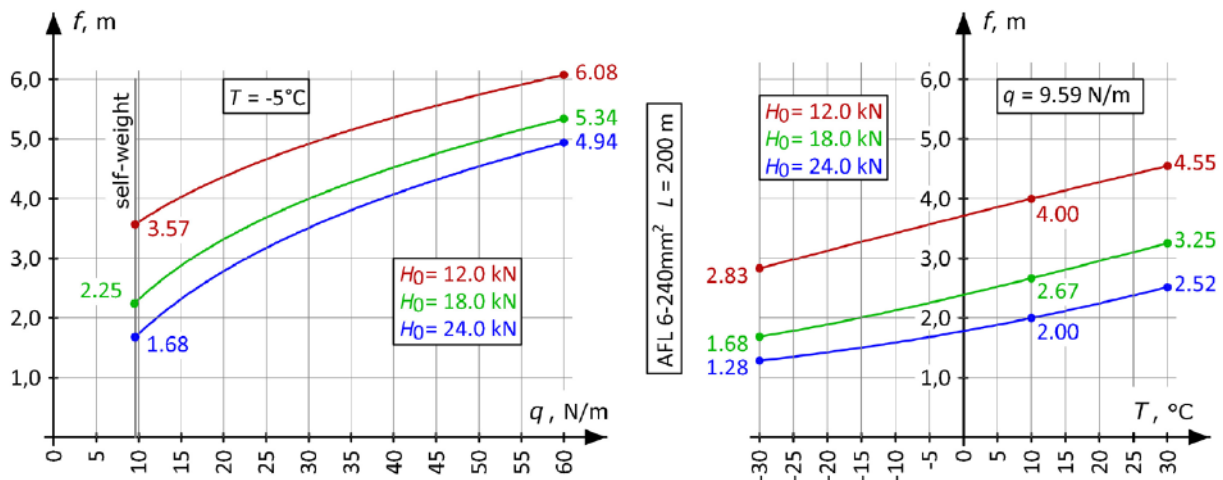


Figure 4. Relationships  $f(q)$  and  $f(T)$  for conductor AFL-6 240 mm<sup>2</sup>

show the shift of the  $H(q)$  graph relative to the origin of the coordinate system (force  $H$  for load  $q$  approaching zero), which serves as a measure of pre-stressing and non-proportionality.

Nonlinearity does not only concern the variability of the tension force  $H$ . The sag of the cable also changes nonlinearly as a function of vertical load  $q$  and temperature  $T$ . Example relationships for the same span  $L = 200$  m are shown in Figure 4.

The nature of the graphs illustrating the effect of vertical load  $q$  on the tension force  $H$  and cable sag  $f$  is similar. Both relationships are curved with a tendency to reduce the rate of increase as the load increases. Additionally, the graphs do not intersect the coordinate system at the origin. Thus, these relationships can be classified as CL-NO (curvilinear, non-homogeneous).

The effect of temperature here is merely illustrative. In the design of power lines, temperature changes are not multiplied by a partial safety factor. Specific states with strictly defined temperatures are considered. As for the impact of icing, it is commonly assumed that its maximum intensity should be associated with a temperature of  $-5^\circ\text{C}$ . Therefore, all the above relationships are presented for exactly this temperature.

### 3.4. Analysis of the $q - H$ relationship

Various measures of nonlinearity are used in the literature to assess deviations from proportionality between action and its effect. For cables, the nature of the relationship is known, and it is understood that the increase in effect (tension force  $H$ ) is slower as the action  $q$  increases.

Firstly, the curvature of the  $H(q)$  graph was assessed. It seems that instead of determining curvature, a simpler and more direct measure of nonlinearity is the **rate of change in force  $\Delta H$  for equal increments in vertical load  $\Delta q$**  (eq. 2). Changes in this rate indicate indirectly the curvature of the relationship between load and tension force:

$$m_t = \frac{\Delta H}{\Delta q} = \frac{H(q_k + \Delta q) - H(q_k)}{\Delta q} \quad (2)$$

This value representing the slope of  $H(q)$  relationship is denoted by the symbol  $m_t$ . Example calculations were performed for a conductor AFL 6-240 mm<sup>2</sup>, in a span of  $L = 200$  m, at a temperature of  $-5^\circ\text{C}$ . Due to use of numerical calculations, the individual values of  $m_t$  were determined assuming an increment  $\Delta q = 0.1$  N/m (with a slope close to the tangent at the point). The result of these calculations is shown in Figure 5.

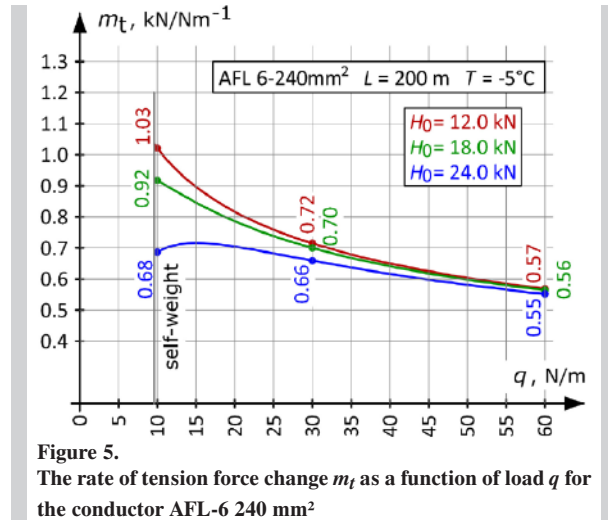


Figure 5. The rate of tension force change  $m_t$  as a function of load  $q$  for the conductor AFL-6 240 mm<sup>2</sup>

For other span lengths, a similar nature of the  $m_t(q)$  relationship is observed. For example, for  $L = 300$  m, the maximum values of  $m_t$  are about 1.35 kN/Nm<sup>-1</sup> (for loads close to the self-weight), while the minimum values are about 0.75 kN/Nm<sup>-1</sup> (for extremely high icing). The results confirm that the discussed relationship deviates from a linear progression.

Another illustration of nonlinearity can be seen in Figure 6. For the same cable, pre-stressed to a force of  $H_0 = 18.0$  kN, the  $H(q)$  curves were determined for different span lengths (200 and 400 m). The calculations were supplemented with tangent lines (slope  $m_t(q_0)$ ) drawn at the starting points of the graphs, corresponding to the self-weight of the cable ( $q_0, H_0$ ). To enhance the readability of the graphs (since the curves share a common starting point), the force change was analyzed at a temperature of  $T = +10^\circ\text{C}$ .

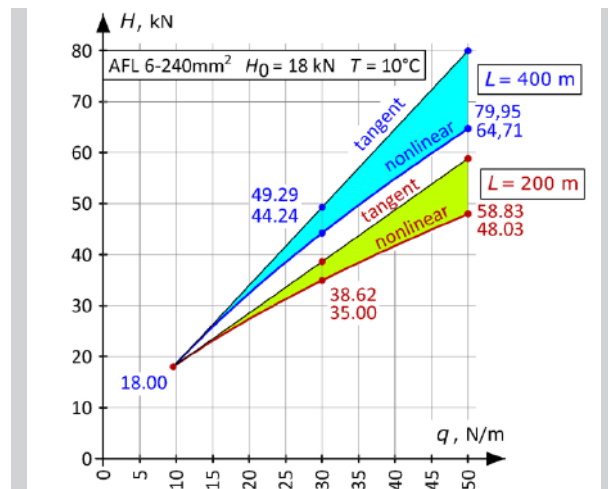


Figure 6. Linearity deviation of the  $H(q)$  relationship for conductor AFL 6-240 mm<sup>2</sup> in spans of 200 and 400 m

The shaded area in Figure 6 graphically illustrates the **curvature of the  $H(q)$  relationship relative to the initial slope of the curve** at the point corresponding to the self-weight of the cable  $q_0$ . The curves that outline the shaded areas (Fig. 6) at the bottom represent results obtained from the cable state equations. The upper boundary is defined by straight lines tangent to the curves at the starting point ( $q_0$ ). The force values were obtained for two different spans,  $L = 200$  and  $400$  m, with an identical pre-tension of  $H_0 = 18.0$  kN. To better assess the analyzed effect, pairs of numerical values are provided at two selected points for each relationship. The smaller values represent the result obtained from the state equations, while the larger values correspond to the result for the linearized relationship. This allows for an evaluation showing that as the distance from the point ( $q_0, H_0$ ) increases, the mentioned difference grows, reaching approximately 10–12% for  $q = 30$  N/m and around 22–23% for  $q = 50$  N/m. Figures 5 and 6 aim to more clearly illustrate the curvature of the variation in tension force  $H$  as a function of load  $q$ , compared to Figure 3.

**3.5. Measures of the nonlinearity of  $q - H$  relationship**

As mentioned in the introduction, the difference between using partial safety factors for actions (approach A) or effects (approach E) is not only due to the curvature of the examined relationship. A second, often more significant factor is the initial pre-stressing of the cable. By applying the load factor  $\gamma$  to the effects (forces), it can be assumed that the  $H(q_k)$  curve is scaled relative to the x-axis, with  $\gamma$  serving as the scaling factor. In this mapping (Fig. 7), each point on the curve for characteristic loads (e.g., point K) corresponds to a higher, scaled effect (e.g., point  $D_X$ ) on the transformed curve. Thus, in approach E, the curve representing characteristic effects (the lower curve) is transformed into the curve representing design effects (the higher curve).

Another way to visualize (Fig. 8) this procedure is to assume that the effect increases proportionally from the origin of the coordinate system. This is graphically represented by a segment starting at point K ( $q_k; H_k$ ) and ending at point  $D_L$ . This segment is part of a straight line  $e$  connecting point K with the origin O. The slope of this line is equal to  $\tan(\alpha_e) = m_e$ . The point  $D_L$ , representing the design (D) value of the effect in the linear (L) approach, is defined by the segment  $KD_L$ , which is  $(\gamma - 1)$  times the length of the segment OK. This visualization makes it easier to compare design values between approaches E and A.

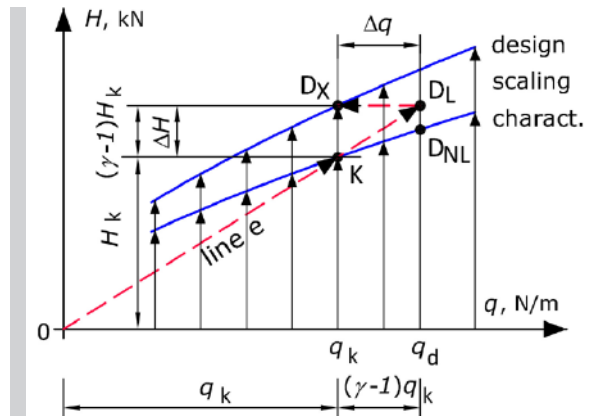


Figure 7. Visualization of the design effects determination method

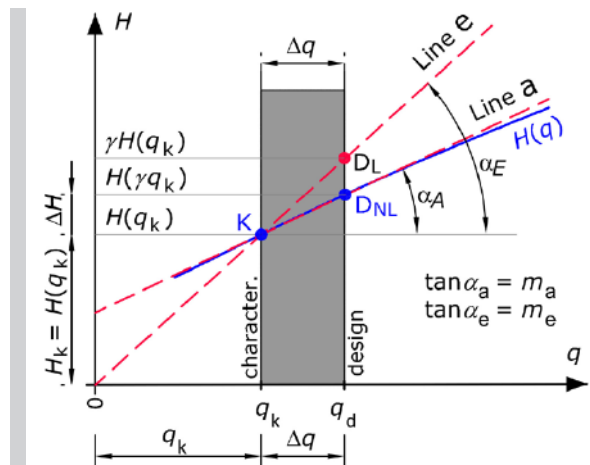


Figure 8. Lines  $a$  and  $e$  (with slopes  $m_a$  and  $m_e$ , respectively) used to determine the force  $H_d$

In approach E, the design value is represented by point  $D_L$  (which has the same effect value as  $D_X$ ). In approach A, corresponding effect is represented by point  $D_{NL}$ , which is located below. This comparison is valid if the load factors applied to actions  $\gamma_A$  and effects  $\gamma_E$  are the same and equal to  $\gamma$ . The mentioned points and procedure are illustrated in Fig. 8.

**3.5.1. Indicator  $n_E$**

In practice, the difference between the design forces  $H_d$  calculated using the nonlinear approach A and the linearized approach E is related to the difference in the slopes of the following two straight lines (see Figure 8):

- The line  $e$  connecting the origin O of the coordinate system to point K ( $q_k; H_k$ ) – with slope  $m_e$ ,
- The line  $a$  connecting points K ( $q_k; H_k$ ) and  $D_{NL}$  ( $q_d; H_d$ ) – with slope  $m_a$ .

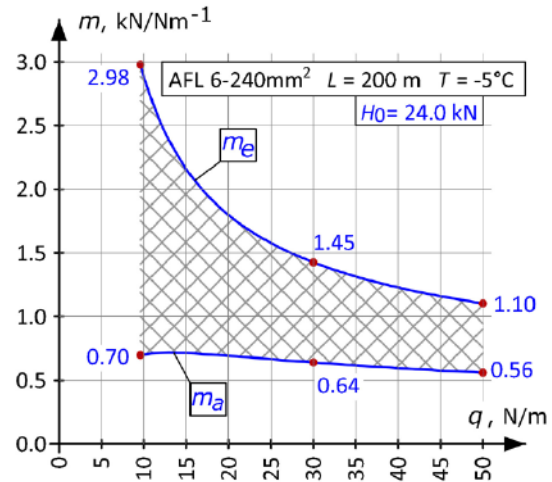
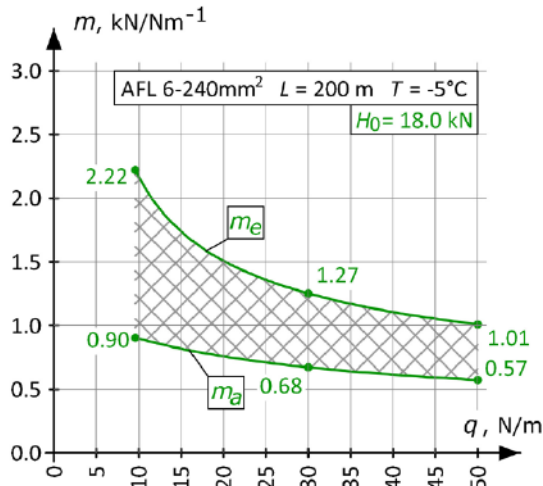


Figure 9. Comparison of slopes  $m_a$  and  $m_e$  for conductor AFL 6-240 mm<sup>2</sup> ( $H_0 = 18.0/24.0 \text{ kN}$ )

The first of the aforementioned lines represents the procedure used in approach E, while the second represents approach A. The measure of nonlinearity can be considered by the indicator  $n_E$ , which is the ratio of the slopes of these lines and is expressed by the following formula:

$$n_E(q_k, \gamma) = \frac{m_e(q_k)}{m_a(q_k, \gamma)} = \frac{H_k/q_k}{\Delta H/\Delta q}, \quad (3)$$

where:

$q_k$  – characteristic load of the cable,

$H_k$  – tension force corresponding to load  $q_k$ ,

$\Delta q$  – increment of load from characteristic to design value:  $\Delta q = q_d - q_k = (\gamma - 1) q_k$ ,

$\Delta H$  – increment of force from characteristic to design value:  $\Delta H = H(\gamma q_k) - H(q_k)$ .

The slopes  $m_e$  and  $m_a$  are functions of the load  $q_k$ . The slope  $m_a$  also depends on the value of the load factor  $\gamma$ . For a specific cable pre-stressed with a force  $H_0$  at a temperature of  $T = -5^\circ\text{C}$ , and with a load factor  $\gamma = 1.3$  (the same for loads and forces), graphs can be generated. These graphs will show the variability of the slopes  $m_e$  and  $m_a$ , as well as the indicator  $n_E$ . The measure of nonlinearity  $n_E$  is calculated as the ratio of these slopes.

The common reference for both methods is point K, representing the solution of the state equation for characteristic loads  $q_k$ . The difference in approaches becomes apparent to the right of this point. By introducing the slopes  $m_a$  and  $m_e$  for lines *a* and *e*, the design values of the tension force can be expressed by the following equations:

$$H_{d,E} = H(q_k) + m_e(q_k)(\gamma - 1)q_k, \quad (4a)$$

$$H_{d,A} = H(\gamma q_k) = H(q_k) + m_a(q_k)(\gamma - 1)q_k \quad (4b)$$

The symbol  $H$  without an index represents the relationship (state equation) used to calculate tension force as a function of load;  $\gamma$  – partial safety factor;  $m_a(q)$  – the slope of the secant connecting points K and D<sub>NL</sub>.

The proportion of the tension force increase  $\Delta H$  between the characteristic and design values can be expressed by the indicator  $n_E$ , which is the ratio of the directional coefficients:

The measure  $n_E$  (eq. 3) is a dimensionless function of the load  $q_k$  and the partial factor  $\gamma$ . Its value indicates whether the effects of the actions grow faster ( $n_E > 1.0$ ) or slower ( $n_E < 1.0$ ) in relation to the actions themselves. A value of  $n_E = 1.0$  is obtained for linear relationships, in which the application of partial factors to both actions and effects leads to the same final result. The indicator  $n_E$ , used here to evaluate the two approaches, has also been used to assess nonlinearity in studies by Uhlemann et al. [13].

An example graph of the variation of the indicator  $n_E$  for AFL-6 240 mm<sup>2</sup> cables in a span of  $L = 200 \text{ m}$ , pre-stressed to  $H_0 = 18.0$  and  $24.0 \text{ kN}$  and  $\gamma = 1.3$  is shown in Figure 10.

The value of the  $n_E$  indicator increases as the directional coefficients  $m_e$  and  $m_a$  differ more for a given load  $q_k$ . For the examined cable, the estimated increase in force  $\Delta H$  (from  $H_k$  to  $H_d$ ) can be more than four times greater with a high pre-tension and



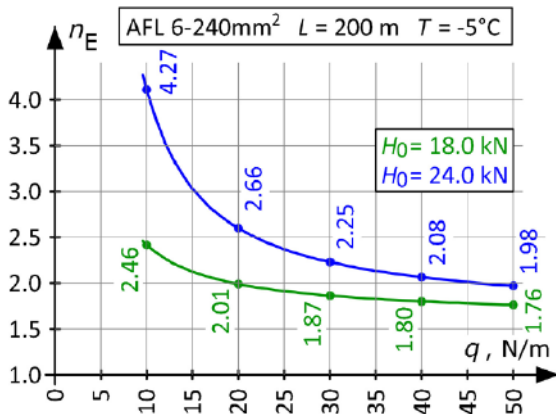


**Figure 10.** Variation of the  $n_E$  for AFL-6 240 mm<sup>2</sup> conductor as a function of load ( $H_0 = 18.0/24.0$  kN)

low loads. This aligns with expectations, as a line  $e$  drawn through a point on the  $H(q)$  graph corresponding to small loads deviates more from the actual relationship. This deviation is distinctly smaller for a large load.

On the other hand, the absolute difference in design forces  $H_d$  obtained by two different approaches also depends on the increase in load values  $\Delta q = q_d - q_k$ :

$$\Delta H = H_{d,E} - H_{d,A} = [m_e(q_k) - m_a(q_k)](\gamma - 1)q_k = [m_e(q_k) - m_a(q_k)]\Delta q. \quad (5)$$

As the load  $q_k$  increases, the mentioned difference also increases, as it is given by  $\Delta q = (\gamma - 1)q_k$ . This fact is symbolized by the width of the shaded area in Fig. 8, which increases with the value of  $q_k$ .

A graphical illustration of determining  $H_d$  for a load of  $q_k = 30.0$  N/m with two different pre-tension forces ( $H_0 = 12.0$  kN and  $H_0 = 24.0$  kN) using two different approaches is shown in Figure 11. The choice of significantly different pre-tensions  $H_0$  was made to better visualize the procedure.

### 3.5.2. Global effect increase factor for approach A

$\gamma_{glob,A}$

Sample calculations were performed, assuming identical values of the load factor for both approaches:  $\gamma = \gamma_E = \gamma_A = 1.3$ . For each of the two examples, triangles (highlighted in Fig. 11) can be identified, with vertices representing the force values:  $H_k$ ,  $H_{d,A}$  and  $H_{d,E}$ . It is evident that for  $q_k = 30.0$  N/m (cable tensioned to  $H_0 = 24.0$  kN), the force  $H_d$  determined

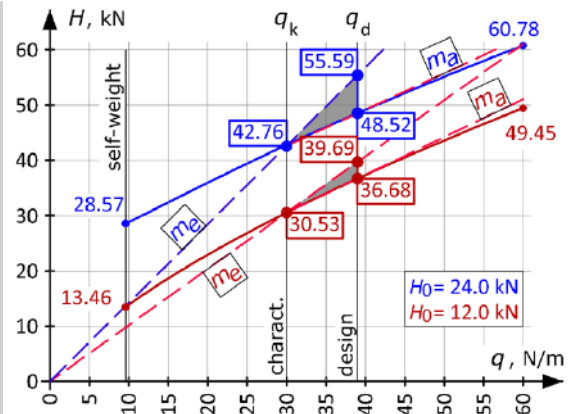


**Figure 11.** Example of determining design tension forces  $H_d$

using approach E is over 7.0 kN greater ( $48.52 \rightarrow 55.59$ ), while for a much smaller pre-tension ( $H_0 = 12.0$  kN) the difference is only 3.0 kN ( $36.68 \rightarrow 39.69$ ). The shaded areas in Fig. 11 indicate the differences in discrepancies. It is clear that the difference in the slopes of the lines  $a$  and  $e$  is significantly larger for the greater initial tension. Similarly, a much larger discrepancy could be observed for lower loads (not shown in Fig. 11).

It should also be noted that by introducing the line  $e$ , one can use a fictitious design load  $q_d$  in the approach E. In practice, such a load is not used. After determining the load  $q_k$  and then the force  $H_k$ , subsequent operations in this approach are carried out solely on the effects (not loads).

All the previously introduced indicators (deviation from linearity, slopes of the lines  $m_e$ ,  $m_a$  and the  $n_E$  indicator) are intermediate measures that ultimately contribute to the final effect. The best measure seems to be the effective global load factor for approach A ( $\gamma_{glob,A}$ ), which can be calculated as:

$$\gamma_{glob,A} = \frac{H_{d,A}}{H_k}. \quad (6)$$

The load factor  $\gamma_{glob,A}$ , as defined above, is introduced specifically to **measure changes in effects within approach A** and is not used in standard procedures. It must be distinguished from the factor  $\gamma_A$ , which is used in this approach solely to amplify actions.

Performing multiple full calculations using numerical methods, it is possible to determine the tension forces that need to be applied to the analyzed supporting structure. For each individual calculation, values such as  $H_k$ ,  $H_{d,E}$ ,  $H_{d,A}$ , as well as the directional



coefficients  $m_e$ ,  $m_a$  and the load increment  $\Delta q$  are obtained. Ultimately, the increase in effect can be assessed using the factor  $\gamma_{\text{glob,A}} = H_{\text{d,A}}/H_{\text{k}}$  and directly compared with the factor  $\gamma_{\text{E}}$  for different data configurations (e.g., cable types, span lengths, pre-tensions, load values). Selected results, including the  $\gamma_{\text{glob,A}}$  values, are summarized in Table 1. When  $\gamma_{\text{E}}$  and  $\gamma_{\text{A}}$  have the same value (1.3 in these considerations), the global factor  $\gamma_{\text{glob,A}}$  can be related to the  $n_{\text{E}}$  indicator by the following relationship:

$$\gamma_{\text{glob,A}} = 1 + \frac{(\gamma_{\text{E}} - 1)}{n_{\text{E}}} = 1 + \frac{0,3}{n_{\text{E}}}. \quad (7)$$

The analysis of the results presented in Table 1 shows that the tension forces  $H_{\text{d}}$  determined using approach A can be significantly lower than those obtained using approach E with the same partial factors  $\gamma_{\text{E}} = \gamma_{\text{A}}$ . For high pre-tension and low loads, the force  $H_{\text{d}}$  may increase by only about 10% with respect to the force  $H_{\text{k}}$ . This discrepancy (10% instead of 30%) arises from the threefold difference in the slopes of lines *a* and *e*. Only with low pre-tension the described increase in effects reach approximately 25%, which is still less than the 30% assumed in approach E.

All previous considerations have been based on the assumption that the partial factors  $\gamma_{\text{E}}$ ,  $\gamma_{\text{A}}$  in both approaches are of the same values. This was done to isolate the single impact, which is the stage of calculations at which factors are applied.

Using partial factors for actions allows for the separation of uncertainties associated with different types of actions. The national annex NNA 2016 [4] recommends using calculation approaches dependent on the type of line (temporary, normal, special). As a consequence, different partial factors are applied for permanent loads and icing. For normal lines, these coefficients are: for self weight –  $\gamma_{\text{G}} = 1.0$  and for icing –  $\gamma_{\text{I}} = 1.25$ . So, the design value of the actions is (approach A/NNA 2016 – subscript A2):

$$q_{\text{d}} = \gamma_{\text{G}} q_0 + \gamma_{\text{I}} q_1 = \gamma_{\text{A2}} q_{\text{k}}, \quad (8)$$

where the total characteristic load amounts to:  $q_{\text{k}} = q_0 + q_1$

In such a case, the equivalent factor for actions is not equal to  $\gamma_{\text{A}} = 1.30$  (Approach A), but for normal lines it is even smaller and equals (Approach A2/NNA 2016):

$$\gamma_{\text{A2}} = \frac{\gamma_{\text{G}} q_0 + \gamma_{\text{I}} (q_{\text{k}} - q_0)}{q_{\text{k}}}. \quad (9)$$

As expected, the value of the  $\gamma_{\text{A2}}$  factor reflects the contribution of permanent loads and ice loads, ranging from 1.0 (when  $q_{\text{k}} = q_0$ ) and increasing with the amount of ice load. Under these assumptions, the design value of the force equals the characteristic value when there is no ice load. As the load  $q_{\text{k}}$  deviates from  $q_0$ , the difference between  $H_{\text{d}}$  and  $H_{\text{k}}$  becomes more pronounced.

#### 4. SAMPLE CALCULATIONS

To summarize the previous considerations and partial results, a broader spectrum of outcomes has been included. These allow for observing how significant the difference can be when different approaches to the application of partial safety factors are employed. The results, which provide a limited sensitivity assessment of  $H_{\text{d}}$  forces calculations, supplemented with nonlinearity indicators, are presented in Table 1.

Sample results of calculating forces  $H_{\text{d}}$  using three different approaches are shown in Figure 12 – on the left for a lower pre-tension  $H_0 = 12.0$  kN, and on the right for a higher  $H_0 = 24.0$  kN. Figure 12 displays four lines, representing (from the lowest line upwards):

- Characteristic forces  $H_{\text{k}}$ ,
- Design forces  $H_{\text{d,A2}}$  determined using varying factors  $\gamma_{\text{G}} = 1.0$  and  $\gamma_{\text{I}} = 1.25$  **for actions**,
- Design forces  $H_{\text{d,A}}$  determined using factor  $\gamma_{\text{A}} = 1.3$  **for actions**,
- Design forces  $H_{\text{d,E}}$  determined using factor  $\gamma_{\text{E}} = 1.3$  **for effects**.

For each graph, the numerical values of forces for three selected load values are provided in the order mentioned above. This allows for a better assessment of the absolute force values characterizing each analysis method.

In conclusion, it should be emphasized that the analyses presented in this article address only a selected aspect (one of several) that causes differences in the effects on overhead electrical transmission towers determined according to the two national annexes NNA 2010 and NNA 2016. A comprehensive analysis of all differences would also need to consider, among other things: varying values of icing effects, different principles for creating load combinations, and reliability levels first defined in NNA 2016. A complete discussion of these aspects goes beyond the scope of this publication.

**Table 1.**  
Sample calculations of forces  $H_d$  and the global factor  $\gamma_{glob,A}$

1	2	3	4	5	6	7	8
$q_k$ N/m	$H_0$ kN	$H_k$ kN	$H_{d,A2}$ kN	$H_{d,A}$ kN	$H_{d,E}$ kN	$n_E$ -	$\gamma_{glob,A}$ -
conductor AFL 6 – 240 mm <sup>2</sup> ; $L = 200$ m; $T = -5^\circ\text{C}$ ; $\gamma_A = \gamma_E = 1.30$ ; $\gamma_G = 1.0$ ; $\gamma_I = 1.25$							
15.0	12.0	18.64	19.84	22.50	24.23	1.45	1.21
30.0	12.0	30.53	34.08	36.68	39.69	1.49	1.20
15.0	18.0	26.08	27.21	29.76	33.90	2.13	1.14
30.0	18.0	37.56	41.05	43.61	48.83	1.86	1.16
15.0	24.0	32.38	33.35	35.59	42.09	3.03	1.10
30.0	24.0	42.76	46.07	48.50	55.59	2.23	1.13
conductor AFL 6 – 240 mm <sup>2</sup> ; $L = 400$ m; $T = -5^\circ\text{C}$ ; $\gamma_A = \gamma_E = 1.30$ ; $\gamma_G = 1.0$ ; $\gamma_I = 1.25$							
15.0	12.0	18.73	20.25	23.73	24.35	1.12	1.27
30.0	12.0	34.67	39.68	43.40	45.07	1.19	1.25
15.0	18.0	27.23	29.09	33.26	35.40	1.35	1.22
30.0	18.0	45.85	51.44	55.54	59.61	1.42	1.21
15.0	24.0	34.58	36.48	40.72	44.95	1.69	1.18
30.0	24.0	53.48	59.12	63.25	69.52	1.64	1.18
conductor AFL 1.7– 70 mm <sup>2</sup> ; $L = 200$ m; $T = -5^\circ\text{C}$ ; $\gamma_A = \gamma_E = 1.30$ ; $\gamma_G = 1.0$ ; $\gamma_I = 1.25$							
10.0	10.0	15.98	17.01	18.19	20.77	2.17	1.14
20.0	10.0	22.87	25.24	26.50	29.73	1.89	1.16
conductor AFL 1.7– 70 mm <sup>2</sup> ; $L = 400$ m; $T = -5^\circ\text{C}$ ; $\gamma_A = \gamma_E = 1.30$ ; $\gamma_G = 1.0$ ; $\gamma_I = 1.25$							
10.0	10.0	18.64	20.37	22.35	24.23	1.51	1.20
20.0	10.0	30.05	33.91	35.95	39.07	1.53	1.20

Results in the columns:

- 1:  $q_k$  – Total characteristic load of the conductor [N/m] ( $q_k = q_0 + q_l$ ),
- 2:  $H_0$  – Initial tension of the conductor at  $T = +10^\circ\text{C}$  [kN],
- 3:  $H_k$  – Force due to the characteristic load:  $q_k$  at  $T = -5^\circ\text{C}$  [kN],
- 4:  $H_{d,A2}$  – Force due to the design load:  $q_d = \gamma_G q_0 + \gamma_I q_l$  ( $\gamma_G = 1.0$ ;  $\gamma_I = 1.25$ ) at  $T = -5^\circ\text{C}$  [kN],
- 5:  $H_{d,A}$  – Force due to the design load:  $q_d = \gamma_A q_k$  ( $\gamma_A = 1.3$ ) at  $T = -5^\circ\text{C}$  [kN],
- 6:  $H_{d,E}$  – Force due to the characteristic load  $H_k$  at  $T = -5^\circ\text{C}$  multiplied by the factor  $\gamma_E = 1.3$ ,
- 7:  $n_E$  – Ratio of the slopes of lines  $e$  and  $a$  calculated using the formula (3)
- 8:  $\gamma_{glob,A}$  – Global safety factor equal to  $H_{d,A}/H_k$  for the approach A.

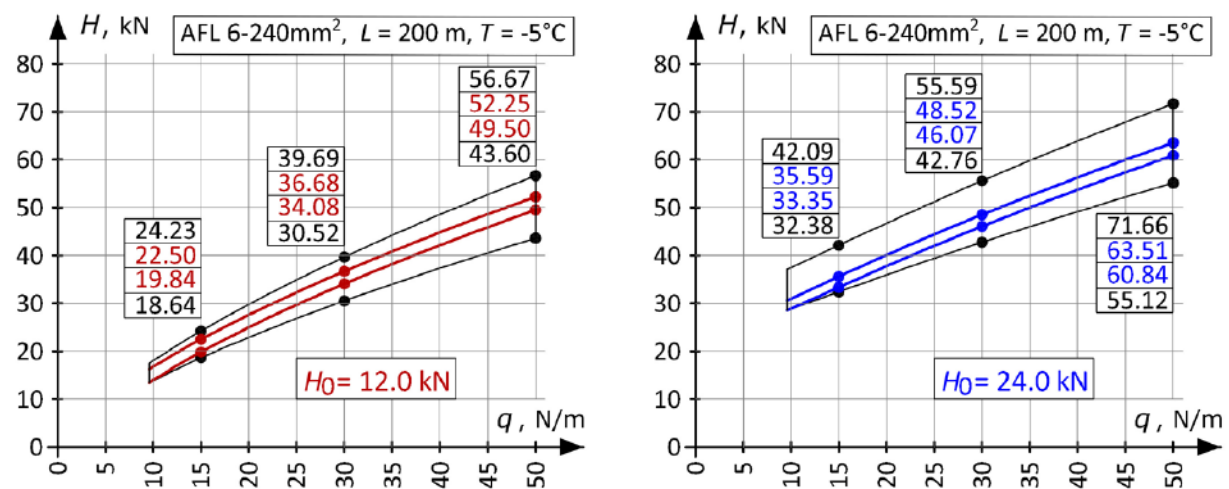


**Figure 12.**  
Tension forces  $H_d$  according to different approaches

## 5. CONCLUSIONS

The method for determining conductor effects on electrical transmission towers significantly affects the resulting forces. Nonlinear phenomena cause variations in computed forces depending on whether partial safety factors are applied to effects or actions. In nonlinear phenomena, it is crucial to specify details to align the approach with the method of partial safety factors (PSF) used in structural design.

In the national annex for Poland to the first edition of the European standard PN-EN 50341-1, the assumption of increasing the effects of loads using partial factors was maintained. This has led to difficulties in separating uncertainties associated with permanent and variable loads, resulting in their treatment as equivalent. While there are interpretations that attempt to make this distinction, they do not stem directly from the standard's provisions but rather from ambiguities in the guidelines provided.

The article focuses on comparing the consequences of applying partial safety factors of 1.3 to loads (before state equation analysis) and to tension forces (after state equation analysis). Most analyses were conducted for a typical 110 kV line conductor with a span of  $L = 200$  m. It was shown that nonlinearity and disproportionate effects of loads lead to varying computed tension forces  $H_d$ , resulting in distinctly different loads on supporting structures.

In analyses using approach A, where the partial safety factor  $\gamma_A = 1.3$  was applied to loads, the computed tension forces  $H_{d,A}$  were determined. To directly compare with approach E, the effect increase was expressed by the factor  $\gamma_{\text{glob},A} = H_{d,A}/H_k$ . This factor allows for a direct comparison of the effect increase and relates it to the factor  $\gamma_E$  used in approach E.

Extensive analyses conducted using proprietary software [7] have shown that the increase in tension force, defined as the rise from the characteristic value  $H_k$  to the design value  $H_d$ , is notably lower in Approach A compared to Approach E. Under extreme conditions (high initial cable tension, low ice load), this increase is only about 10%. In average conditions, the increase is expected to be around 20%.

Considering the varying values of partial factors assigned to permanent and variable actions in Approach A according to NNA 2016 (with their values simultaneously less than 1.30), the design tension force  $H_d$  can be, in extreme situations (at the lowest levels of ice load), only 5-6% greater than force  $H_k$ . Detailed results for the selected data can be reviewed

in the tables and figures presented in the article.

The analysis also identifies the reasons for discrepancies between the approaches considered. These discrepancies arise from different methods of estimating the effects of increased load, which are expressed by the slope of the lines estimating the change in effect (tension force) relative to the cause (load). Among the two causes of nonlinearity (curvature of the  $H(q)$  relationship and disproportionality of increases  $\Delta H/\Delta q$  due to pre-tension, i.e., offset from the origin of the coordinate system), the second has a greater impact on the final result discrepancies between approaches A and E.

It is worth noting that shifting from approach E to approach A is rational due to the adjustment of safety margins proportional to the uncertainties associated with different types of loads. Although approach E is simpler to implement, it can lead to unreasonable overestimation of design forces in some cases. This is evident from a simple analysis of the  $H(q)$  relationship, which shows that a 30% increase in force  $H$  requires a significantly larger increase in load. This conclusion is based on sample calculations of indicators determining the rate of change in effect relative to cause.

The example presented in the article highlights the significance of the examined effect. Extending and generalizing the conclusions to other configurations of power lines is only partially justified. In real terms, the forces applied to the structure are also influenced by factors such as the method of determining the characteristic ice accretion load, standard combinations (e.g., related to uneven accretion), differences in span lengths on either side of the tower, and the angle of the route bend, etc.

In summary, Approach A leads to a reduction in the  $H_d/H_k$  force ratio (compared to Approach E). Although Approach A increases the workload due to the need to repeatedly solve state equations, it aligns better with the concept of differentiating safety factors according to the uncertainty in determining various action values. However, it should be also noted that the discussed issue of applying PSF only partially explains the differences in determining conductor actions according to the NNA 2010 and NNA 2016 national annexes.

## ACKNOWLEDGEMENTS

The development work for the UMKW system was funded under grant no. POIR.01.01.01-00-0792/17 by the National Centre for Research and Development (NCBiR), Operational Program Intelligent Development 2014–2020, action 1.1/sub-action 1.1.1.



## REFERENCES

- [1] CENELEC. Standard EN 50341-1:2005 Overhead electrical lines exceeding AC 45 kV Part 1: General requirements - Common specifications.
- [2] CENELEC. Standard EN 50341-1:2012 Overhead electrical lines exceeding AC 1 kV Part 1: General requirements - Common specifications.
- [3] PN-EN 50341-3-22:2010 Overhead electrical lines exceeding AC 45 kV. Part 2: Set of National Normative Aspects (NNA) for Poland, PKN 2010.
- [4] PN-EN 50341-2-22:2016 Overhead electrical lines exceeding AC 1 kV. Part 2: Set of National Normative Aspects (NNA) for Poland, PKN 2016.
- [5] Wandzik G. (2015). Design of power lines in Europe seen through the prism of national normative annexes to the EN 50341 standard. VI Scientific-technical Conference: Overhead Power Lines, Wisła 2015 (in Polish).
- [6] Kapłański G., Kowalczyk G., Szojda L., Wandzik G., Włodarczyk K. (2022). Universal Modular Support Structures (UMKW) as an Alternative for Power Transmission in Emergency Situations. 30 Conference on Structural Failures, Międzyzdroje 2022 (in Polish).
- [7] Wandzik G.: UMKW – Line (2023). Computer software for the analysis of conductors and loads on overhead line support structures According to the PN-EN 50341, Gliwice, 2020-2023.
- [8] Bakeer T. (2022). The theory of homogeneity of non-linear structural systems. A general basis for structural safety assessment. <https://arXiv: 2212.01423>.
- [9] CEN, Standard EN 1990:2010 (Eurocode 0) : Basis of structural design. Brussels, 2010.
- [10] Gulvanessian H., Calgaro J.-A., Holicky M. (2012). Designers' Guide to Eurocode EN 1990: Basis of structural design. ICE Publishing; 2<sup>nd</sup> edition, Thomas Telford Limited, London 2012.
- [11] Ditlevsen O., Madsen H.O. (2007). Structural Reliability Methods Department of Mechanical Engineering, Technical University of Denmark, Copenhagen, Internet Edition 2.3.7.
- [12] Eibl J. (1996). Nonlinear design and an appropriate safety format. IABSE Rep., vol. 74, Delft: International Association for Bridge and Structural Engineering; 1996. <https://doi.org/10.5169/SEALS-56066>.
- [13] Castaldo P., Gino D., Mancini G. (2019). Safety formats for non-linear finite element analysis of reinforced concrete structures: discussion, comparison and proposals. *Eng Struct*; 193, 136–53. <https://doi.org/10.1016/j.engstruct.2019.05.029>.
- [14] Teichgräber M., Fußeder M., Bletzinger K.-U., Straub D. (2023). Non-linear structural models and the partial safety factor concept. *Structural Safety* (103). <https://doi.org/10.1016/j.strusafe.2023.102341>.
- [15] Fusseder M, Teichgräber M, Bletzinger K, Straub D, Goldbach A (2021). Investigations on the design of membrane structures with the semi-probabilistic safety concept. 10<sup>th</sup> Ed. Conf. Text. Compos. Inflatable Struct., CIMNE; 2021. <https://doi.org/10.23967/membranes.2021.011>.
- [16] Uhlemann J., Stimpfle B., Stranghöner N (2014). Application of the semiprobabilistic safety concept of EN 1990 in the design of prestressed membrane structures. In: Proceedings of the EUROSTEEL. 2014.
- [17] Stranghöner N, Uhlemann J, Bilginoglu F, Bletzinger K-U, Bögner-Balz H, Gerhold S, et al. (2016). Guideline for a European Structural Design of Tensile Membrane Structures Made from Fabrics and Foils-. Background documents in support to the implementation, harmonization and further development of the Eurocodes.
- [18] Cigre Technical Brochure No 324 (B2.12.3): Sag-Tension Calculation Methods for Overhead Lines. Cigre, June 2007.
- [19] CEN, Standard EN 1993-3-1:2008, Eurocode 3: Design of Steel Structures. Part 3.1: Towers, Masts and Chimneys, Brussels, 2008.
- [20] Mendera Z., Szojda L., Wandzik G. (2012). Steel Support Structures for Overhead Power Lines. Wydawnictwo Naukowe PWN SA, Warszawa (in Polish).
- [21] Mendera Z., Szojda L., Wandzik G. (2017). Design of Steel Towers for Overhead Power Lines in the Context of European Standards. Wydawnictwo Naukowe PWN SA, Warszawa (in Polish).